A 350 Micron Array Polarimeter Using Translational Modulators

David T. Chuss[a], Dominic J. Benford[a], Chris Walker[c], S. Harvey Moseley[a], Giles Novak[b], Johannes G. Staguhn[a], and Edward J. Wollack[a]

[a]NASA Goddard Space Flight Center, Code 685, Greenbelt, MD, USA;
[b]Northwestern University, Department of Physics and Astronomy, Evanston, IL, USA
[c]University of Arizona, Tucson, AZ, USA

ABSTRACT

We describe a polarimeter that will be a testbed for a novel polarization modulator. This modulator is composed of two modified Martin-Puplett interferometers in which the input polarization state is transformed by adjusting the phase delays between linear orthogonal polarizations in each of the two stages. This type of modulator represents a potential improvement over existing technology in the following three ways. First, these modulators can fully characterize the polarization state by measuring Stokes Q, U, and V. The characterization of V is especially useful as a diagnostic for systematic errors. Second, the Martin-Puplett modulators can be easily retuned to observe at multiple frequencies. Finally, the small translations required for modulation can be accomplished with fewer moving parts than the rotational motions in wave plate modulators, thus potentially leading to modulators with longer lifetimes than those currently employed in polarimeters. The next generation of polarimeters, designed for both the study of Galactic magnetic fields in the far-infrared and submillimeter and the measurement of the polarized component of the Cosmic Microwave Background, will need to incorporate modulators with these attributes.

This prototype polarimeter will be a modified version of the Hertz polarimeter that had until recently been operating on the Caltech Submillimeter Observatory. After modification, Hertz will be moved to the Heinrich Hertz Telescope in Arizona. We will utilize dynamic scheduling to efficiently observe during the best fraction of weather at this site.

Keywords: Submillimeter Polarimetery, Astronomical Instrumentation

1. INTRODUCTION

New detector technologies have recently found broad astronomical applications from the far-infrared through the millimeter parts of the electromagnetic spectrum. New instruments from SOFIA[1] to ACT[2] will employ different implementations of bolometer technologies that span the wavelength range from 30 to 3000 μm. Polarimetry at these wavelength is also of scientific interest, and in the next few years, both far-infrared(FIR)/submillimeter and millimeter polarimetry will be the focus of many new instrument development efforts. The next generation of instruments for each field shares a common set of scientific and technical requirements, and thus it is advantageous to examine the problems in parallel, to the extent possible.

In recent decades astronomers have been able to gather an abundance of stunning images and detailed spectra towards star forming regions. These investigations have been made from space as well as from the ground, and have revealed not only large numbers of protostars, but also a variety of phenomena associated with their birth, such as accretion and proto-planetary disks, bipolar outflows and jets, and turbulent as well as shocked gas in the protostellar environs. Meanwhile, advances in techniques for numerical simulation are allowing ever more realistic simulation of the complex physical processes involved.[3]

Despite these advances, definitive explanations have not been found for observables like the initial mass function and the star formation efficiency. One important gap in our observations is the magnetic field. It has

Further author information: (Send correspondence to D.T.C.)
D.T.C.: E-mail: chuss@stars.gsfc.nasa.gov, Telephone: 1 301 286 1858

long been recognized that interstellar magnetic fields are frozen into the gas out of which stars form, and that these fields are strong enough to affect the process.[4] For example, the fields may affect the formation of giant molecular clouds, via the magneto-rotational instability.[5] A popular theoretical idea holds that static magnetic fields provide support against gravity in low-mass star forming regions.[6] This idea would seem to explain the low star formation efficiency inferred for these regions, but it has been called into question in recent years.[7] Finally, in the later stages of the star formation process, it seems likely that magnetic forces are responsible for driving jets and outflows[8] which in turn may be important for angular momentum transfer and accretion rate. But interstellar fields are difficult to observe, and the available observations have not been conclusive in terms of their connection to theory.[9]

The alignment of interstellar dust grains by Galactic magnetic fields, discovered in 1949, allows astronomers to map out the direction of a cloud's magnetic field.[10] More specifically, what is measured is the orientation of the projection of the magnetic field onto the plane of the sky. There are two somewhat distinct methods that both rely on grain alignment to map fields. The first is polarimetry of optical and near-IR light from background stars that becomes polarized by selective extinction as it passes through a medium of aligned grains.[11,12] The second is far-IR/submillimeter polarimetry of thermal emission from aligned grains, which is also polarized. This second method was established during the 1980's[13,14] and has two big advantages over the first method. First, any sight-line can be sampled, even if no background star is present. Second, the possibility of polarization by scattering can be generally discounted because the wavelength is much longer than the grain dimensions. The emission is usually optically thin, which simplifies the interpretation. Polarized thermal emission has by now been detected in scores of clouds.[15,16]

Because of the recent dramatic improvements in technology for IR and submillimeter observations, it appears likely that significant advances in understanding the role of magnetic fields in star formation will come from polarimetry of thermal emission from dust. One important technological development is the explosion in bolometer-array technology. Even as instruments with dozens of pixels are still being operated, thousand-pixel instruments are now under construction, and even larger arrays are likely to be available by the end of the decade. Equally important are new and larger telescopes such as ALMA, SOFIA, and the Large Millimeter Telescope (LMT), new and dryer telescope sites like South Pole and Atacama, and eventually a space platform for far-IR polarimetry. As the telescopes become more remote and the instruments become more expensive and complex, it becomes crucial for polarimetric instrumentation to incorporate modulator technology that allows good control of systematics, is flexible in frequency coverage, and has a high reliability.

Submillimeter continuum polarimetry using ALMA and the use of thousand-pixel detectors on large single-dish telescopes will lead to vast increases in our knowledge concerning the configuration of magnetic fields in molecular clouds, star forming cores, infall envelopes, and accretion disks. However, there are two important challenges facing such observations: (i) differing magnetic geometries of different cloud components superposed along a single line-of-sight will not be easy to separate, and (ii) the observations will be restricted to regions of high column density. The first limitation arises because submillimeter continuum observations, unlike spectral line observations, cannot discriminate between different gas components based on their line-of-sight velocities. Submillimeter continuum polarimetry is sensitive to all grains along a given line-of-sight, leading to difficulties in unambiguously assigning magnetic field directions to different spatial regions within a given cloud. For the second point, systematic effects limit the polarimeter's sensitivity to a particular fraction of total power on the detectors. In order to extend observations to fainter astronomical sources, either one must decrease the background loading on the detectors by building a space-based polarimeter, or one needs to increase the control over systematics. The former is a viable option for FIR observations; however, telescope size restrictions make this option unrealistic in the submillimeter. Thus, in order to complement future space-based FIR polarimetric observations, systematic errors must be reduced for the next generation of ground-based polarimeters. This reduction will be complemented by large-format arrays that will make possible the longer effective observing times required to reach the statistical limits necessary to take advantage of such systems.

At longer wavelengths, polarimetry of the Cosmic Microwave Background (CMB) is currently one of the most active fields of astronomy due to its potential for significantly advancing our the understanding of the early universe. Discovered in 1965,[17] the CMB is the signature of the surface of last scattering. This corresponds to the redshifted spectrum of the universe as it appeared 380,000 years after the big bang (z=1089)[18] when

radiation decoupled from the baryons. Today, we observe the surface of last scattering as a spatially uniform 2.73 K blackbody[19] to one part in $\sim 10^5$. As such, the CMB is the oldest picture we currently have of the universe. The primary anisotropy, which exists at a level of $\sim 10^5$ below that of the total power of the CMB, provides important information as well. Believed to be a result of quantum fluctuations that were stretched to macroscopic scales by inflation, the statistical properties of the anisotropy have been able to provide details of the physical properties of the universe including its age, geometry, and relative abundances of baryons, photons, dark matter, and dark energy.[18]

Because the primary anisotropy produces a quadrupole moment in the energy distribution at this surface of last scattering, Thompson scattering is expected to produce a polarization pattern that is anti-correlated with the anisotropy and was discovered to be at the level of $\sim 10^6$ below the 2.73 K blackbody signature.[20] The polarization signals that arise as a result of the quadrupole moment of the primary anisotropy are curl free and are referred to as "E-Modes." In addition to these E-modes, quadrupole anisotropies in the surface of last scattering can result from gravitational waves produced from the stretching of vacuum fluctuations during inflation. These polarization signals have a curl component and are thus dubbed "B-modes." These B-modes are of great interest because their magnitude (expected to be $\sim 10^{-7}$ to 10^{-9} of the total flux) is a measurement of the energy scale of inflation.

The instrumentation challenges presented by these two scientific problems are similar. The problem in both cases is to measure a polarized signal that is a small fraction of the total power incident on a detector. In the case of submillimeter polarimetry, one attempts to detect fractional polarizations of the order of a few percent of source fluxes while looking through an atmosphere that provides a significant amount of flux to the detectors. For the CMB case, the majority of the power comes from the CMB itself, with the polarization signature being a small fraction of the 2.73 K blackbody. In the case of submillimeter polarimetry, the ratio of polarized flux to total flux is about 10^{-6} (see Appendix). This is the same approximate level of precision of current measurements of E-mode polarization. Better control over systematics in each case can lead to increases in sensitivity to fractional polarization. In the case of FIR/submillimeter polarimetry, this involves measuring polarizations in fainter regions ($A_V < 10$). In the CMB case, increased sensitivity allows one to approach the level of the B-modes.

One way to increase one's understanding of the systematics of a polarimeter is to provide the capability to measure circular polarization in addition to linear. Theoretical estimates place the level of circular polarization due to dust grain-radiation interaction at 10^{-4} of the linearly polarized flux.[4] If this is true, the measurement of circular polarization significantly above this level will provide valuable information about the instrument's cross-polar response that otherwise would be unknown. Similar issue confronts those interested in measuring the B-modes of polarization of the Cosmic Microwave Background. For the B-modes, it is expected that the linear polarization signal be 10^{-7} to 10^{-9} times smaller than the unpolarized part of the signal. Because of this, improvement in control of systematics over the current state of the art is necessary. In this case, the circular polarized component is also expected to be much lower than the linear polarization component ($\sim 10^{-12}$ times the total power at 100 GHz).[21] Thus, sensitivity to circular polarization can provide an important calibration.

Both FIR/submillimeter and CMB polarimetry will require observations at multiple frequencies. In the case of FIR/submillimeter polarimeter, multiple bands will provide the ability to separate regions of different temperatures along the line of sight. The range of wavelengths that will be made accessible first by SOFIA, roughly 30-300 μm, corresponds to the thermal emission peaks of grains with temperatures ranging from 300 K to 30 K. This will complement the capabilities of the submillimeter polarimeters which will allow only limited temperature separation. For the CMB, multiple bands are required to separate Galactic foreground effects from those intrinsic to the CMB.

Finally, in order to maximize the effectiveness of instruments in both areas of study, space-based telescopes are required. For FIR polarimetry, spaced-based missions allow for the elimination of the large background signals due to the opacity of the atmosphere that is inherent for both ground-based submillimeter observatories and airborne FIR facilities. Decreased background loading allows for greater sensitivity of the detectors, and it increases the ratio of polarized to total flux. For the CMB, a satellite mission eliminates atmospheric effects. In addition, it allows for full sky coverage which greatly improves the statistical analysis of the CMB angular spectrum. Such space missions will require reliable modulator technologies

New polarization modulators based on a dual Martin-Puplett interferometer architectures[22] are a viable candidate technology for the next generation of polarimeters. These modulators work in reflection and allow the phase delay between orthogonal polarization states to be dynamically adjusted. Because of this fact, they can fully characterize the polarization state of incoming radiation, measuring circular as well as linear polarization. They can also easily be retuned for multiple frequencies. Finally, their minimization of the complexity of moving parts makes them ideal for space missions.

We describe a proposed polarimeter that will be a testbed for this candidate technology. We will use the University of Chicago's Hertz polarimeter[23] and the University of Arizona's Heinrich Hertz Telescope (HHT) to construct a 350 μm polarimetric measurement system.

In section 2, we describe the polarization modulators, including their design, details concerning future laboratory testing, and proposed observation modes. In section 3, we outline the plans for data acquisition and analysis. In sections 4 and 5 we present brief descriptions of the HHT and the Hertz polarimeter, respectively. Finally, we conclude with a brief summary.

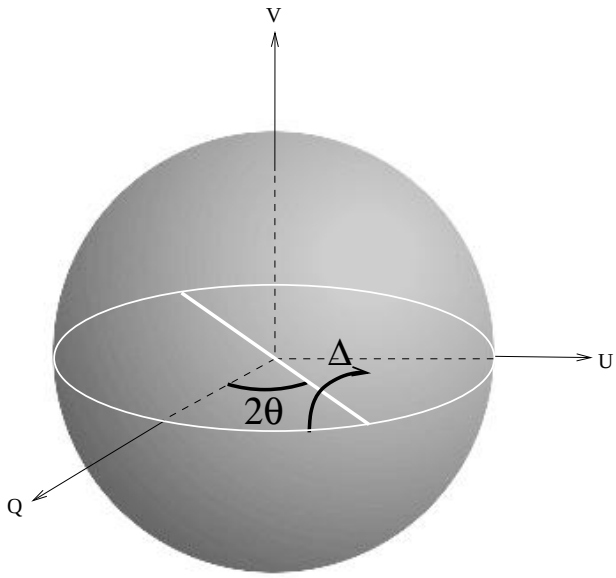

Figure 1. The Poincaré sphere is a surface of constant polarization in a space having Stokes Q, U, and V as coordinate axes. A polarization modulation in this space is represented by a rotation. Here, a phase delay, Δ, is introduced between polarization states represented by the points of interesection of the white line and the surface of the sphere.

2. POLARIZATION MODULATORS

2.1. Architecture

The polarization state of incoming light can be completely described by four numbers called Stokes parameters. These are represented by (I, Q, U, V). I is simply the total intensity, Q and U are quantities that describe the linear polarization of the light, and the circular polarization is described by V. An ideal modulator changes the polarization state of the incoming radiation. That is, it rearranges the power present in Q, U, and V without changing the polarization,

$$P^2 = Q^2 + U^2 + V^2$$

or the total intensity, I.

A useful way to visualize the action of a modulator is through the use of the Poincaré sphere. The Poincaré sphere, shown in Figure 1, lies in a space that has as its axes Q, U, and V. The surface of the sphere is the set of all polarization states having a common polarization. Linearly polarized states are those that lie on the equatorial circle, circular polarization states lie at the poles, and all other points on the surface represent elliptically polarized states.

Since a perfect modulator is only allowed to change the polarization state, leaving the total polarization unaffected, the action of a modulator can be represented by a rotation in Poincaré space. In Figure 1, the white line shows a possible axis of rotation. This axis is defined as the diameter connecting two orthogonal polarization states between which a phase, Δ, is introduced. The magnitude of the phase delay gives the amount of rotation.

Though it is possible to imagine a rotation about any axis on the Poincaré sphere, we restrict the discussion here to axes that lie in the $Q - U$ plane. The reason for doing this is that most physical modulators rely on introducing a phase delay between two orthogonal linear polarizations. Figure 1 shows the effect of introducing a phase delay Δ between orthogonal linear polarization components, one of which is oriented at an angle θ with respect to the Q axis. This is exactly the action of a half-wave plate. In this case, the phase difference is fixed at $\Delta = \pi$, and the plate is allowed to rotate thereby changing θ.

It is also possible to fix θ and instead vary Δ. In this case, two modulators are required to map an initial state into an arbitrary new state, as navigation on the two-dimensional sphere surface requires two coordinates.

A modified Martin-Puplett architecture can be used to introduce a phase delay between two orthogonal linear polarization components.[22] Figure 2, the grid is oriented with its wires at 45° relative to the axes of the rooftop mirrors. Each arm of the interferometer carries an orthogonal linear polarization such that the phase difference between them can be modulated by adjusting the relative distance of each arm. The introduced phase difference is simply $\Delta = 4\pi(d_2 - d_1)/\lambda$. Here, λ is the wavelength of the light being modulated. For a phase difference $\Delta = \pi$, the interferometer will reflect the linear polarization of the incoming radiation about the axis defined by the grid. For example, if the incoming transverse electric field vector is oriented at at angle ϕ with respect to the grid wires, the outgoing field vector will have an angle $-\phi$.

In order to provide the ability to access any point on the Poincaré sphere, two degrees of freedom are necessary. Thus, two serial Martin-Puplett interferometers are required for complete modulation. The first is oriented at an angle of 22.5° and the second is oriented at an angle of 45° with respect to the chosen reference axis that defines Q. Generally, the Q-axis is defined by the orientation of the detectors. Toggling the first interferometer's phase delay between 0 and π selects which linear Stokes parameter is being measured at the detectors. Toggling the second switches the sign of the selected Stokes parameter. (See Table 1.) A proposed architecture for a full submillimeter modulator is shown in Figure 3. In this architecture the action of each Martin-Puplett stage is performed by a series of two reflections that separate the polarization components. The grid-mirror pairs in each of the two stages introduce phase delays between orthogonal components of polarization.

2.2. Laboratory Testing

A large fraction of the effort of building this instrument will be invested in the development of a modulator having systematic effects that are low and well understood. For this reason, laboratory testing of the device is important. We will build a prototype single Martin-Puplett modulator to guide us in the design of the device to be used at the telescope.

The two general classes of effects we want to measure in the lab tests are as follows. First, we want to know the transmission of the device. This can be a polarized or unpolarized response and will tell us how close the actual modulator conforms to the condition that the total polarized power remains constant through the device. The quantity that summarizes this class of effects is the coupling or leakage of Stokes I into the other three Stokes parameters. In Poincaré space, these effects manifest themselves as translations normal to the surface of the sphere. The other class of effects in which we are interested concern the polarization transfer function. Here we are looking for deviations from the predicted rotations in Poincaré space.[22] Because of imperfections in the device, we expect some additional leakage of one polarization into another.

Specifically, we wish to characterize and asses the effects of various systematics that are possible in such a setup. First, as the beam propagates through the modulator, part of the beam may spill off of the edge of

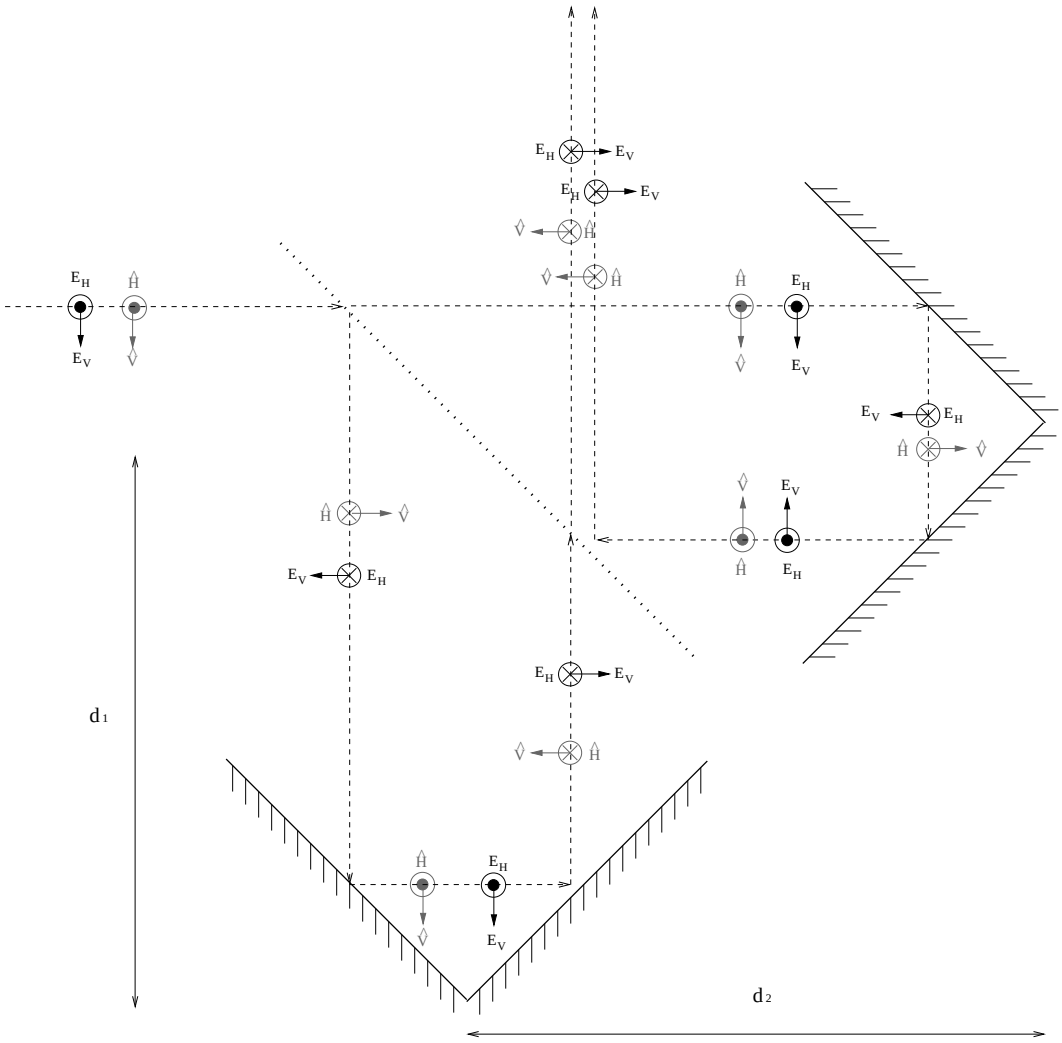

Figure 2. A single modified Martin-Puplett interferometer is shown. The interferometer introduces an adjustable phase delay between two orthogonal polarization states, each of which propagates through a separate arm of the interferometer. For zero phase delay ($d_1 = d_2$), this device has an identical transformation to that of a mirror. The propagation of both the electric fields and the $(\hat{H}, \hat{V})$ coordinate system through the device is shown.

the rooftop mirrors. This effect will manifest itself as a loss of efficiency in the system's throughput, and it is advantageous to understand this. However, if the amount of spillover changes with modulator position, a spurious polarization signal may arise. Similar effects can result from misalignments between the grids and mirrors of the interferometer. Finally, since the goal is to design a system that can accommodate all of the beams from the elements of a detector array, it is vital to understand the modulator's response to beams that enter the device at angles that deviate from normal incidence.

2.3. Observing Modes

The initial observing strategy is based on techniques developed for array polarimetry.[24] This involve a strategy involving "chopping" the telescope's secondary mirror to subtract the effect of changing atmospheric opacity coupled with a lower frequency "nodding" in which the source is alternatively placed in the left and right beams as defined by the chopping modulation. Nodding reduces synchronous offsets produced by temperature gradients across the primary. This technique will also reduce the effect of polarization offsets resulting from

polarized emission gradients across the primary. For polarimetry, both nodding and chopping are performed at each modulator position. For the dual Martin-Puplett modulators, two modulator settings are required for each of Q, U, and V.

The simplest mode of operation in which this modulator can measure the polarization state of incoming light. This mode of operation is similar to that used for a half-wave plate. It is helpful to imagine that the detector is sensitive to Stokes Q in the absence of modulation. Such a "detector" can be realized by placing a polarizing grid in the beam path and using bolometers to measure both the transmitted and reflected radiation from the grid. The difference in the two signals is a measure of Stokes Q. The role of the modulators in the light path from the detector to the sky is to rotate this point around the Poincaré sphere to generate enough measurements to fully characterize the polarization. Recall that in order to measure the linear Stokes parameters, Q and U, the two modulators are placed such that the wires of their polarizers make angles with respect to the axis defining Stokes Q of 22.5° and 45°, respectively. The phase lags introduced between the two polarizations at each of these modulators are varied between 0 and π (no retardation and half-wave retardation, respectively). The detector is then mapped onto the sky as illustrated in Table 1.

As one can see in Table 1, toggling the first Martin-Puplett between 0 and π has the effect of switching between Stokes Q and Stokes U. Toggling the second Martin-Puplett switches between a linear Stokes parameter and its opposite polarization (the opposite point on the diameter of the Poincaré Sphere.) In a similar fashion, circular polarization (Stokes V) can be measured by setting the first interferometer to a phase delay of zero and toggling the second between $\pi/2$ and $3\pi/2$.

Table 1. Simple Modulation Scheme for a Dual Martin-Puplett Modulator

MP1(22.5°)	MP2(45°)	Quantity Measured
0	0	Q
0	π	$-Q$
π	0	U
π	π	$-U$
0	$\pi/2$	V
0	$3\pi/2$	$-V$

During the second season of operation, once the initial goal of obtaining astronomical data with this instrument is achieved, we will experiment with strategies involving the continuous scanning of the modulators. Such strategies are expected to increase the effective efficiency of the modulator over the passband of interest. In addition, sinusoidal operation of the transports can be an effective way to minimize power consumption for space missions that have constraints on the total power usage.

3. DATA SYSTEM

There is currently a funded effort underway to add polarimetric capability to SHARC II at the Caltech Submillimeter Observatory.[25] To the extent possible, Hertz/HHT will conform to the techniques and standards set by this polarimetry system. This will avoid duplication of effort and will provide a larger knowledge base for technical issues that will be encountered. For the data acquisition system, we will copy that of SHARC II.[26] This involves building an optical fiber interface board to mate the optical fibers from the existing Hertz external electronics to a commercial DSP board mounted in a VME bus of a SPARC computer. We will use the existing driver software for the software interface. For software control, we will use the IRC (Instrument Remote Control) developed at NASA/GSFC.[27] All required demodulation will be accomplished in software.

4. HEINRICH HERTZ TELESCOPE

The Steward Observatory 10 m Sub-Millimeter Telescope Observatory (SMTO) is situated on Mount Graham in Arizona. The winter and spring months (November through April) generally bring the best submillimeter

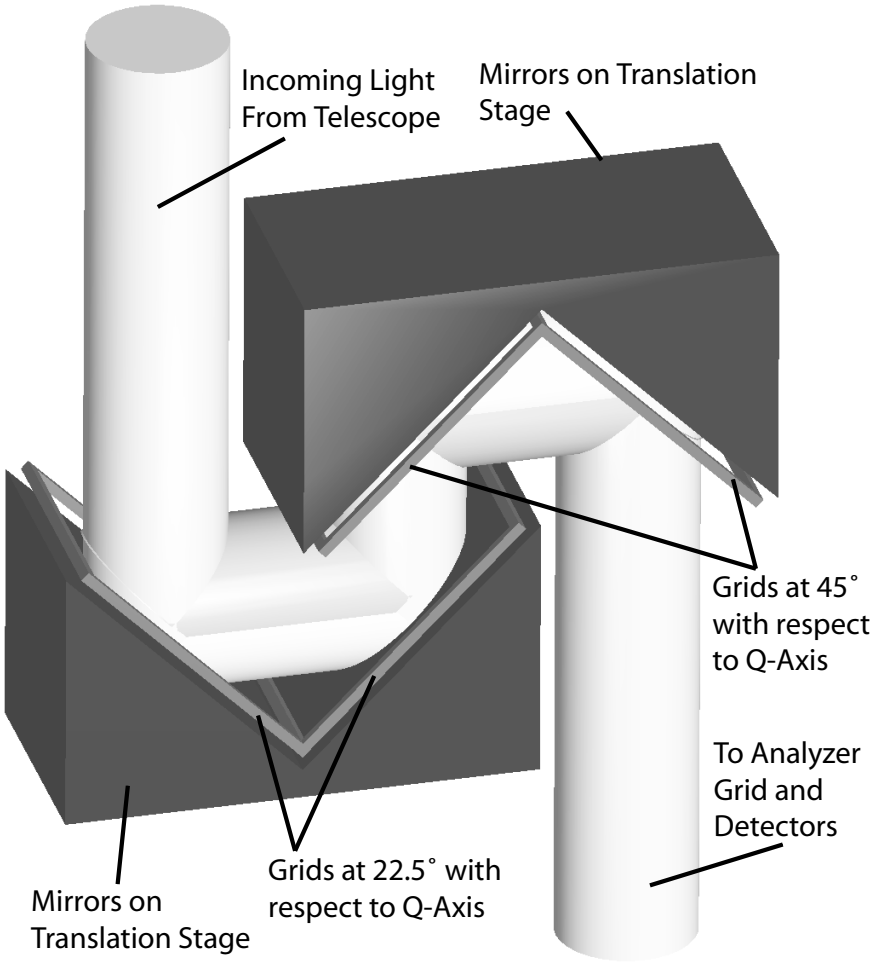

Figure 3. The design concept for a submillimeter modulator is shown. The first set of grids in the optical path has wires that are oriented at an angle of 22.5° with respect to reference (Q) axis. The second set has wires oriented at a 45° angle. The mirrors are mounted on translational stages and each is moved to adjust the relative phase of the two polarization states that are separated by the grids.

observing conditions at the site with an optical depth τ at 225 GHz of less than 0.06 typically 10%-30% of the time. The SMTO will be available for dynamically scheduled astronomical observations with the Hertz polarimeter in order to take advantage of the best available weather conditions.

5. HERTZ POLARIMETER

The University of Chicago's Hertz polarimeter[23] is a 350 μm array polarimeter. It has two arrays of 32 pixels arranged in a 6×6 square with the corners removed. The dual arrays measure the horizontal and vertical linear polarization components of the incoming radiation. This allows for the reduction in noise due to time variation of the atmospheric opacity. This "sky noise" is correlated in each of the arrays and can be nearly eliminated by subtracting the two components.[24]

The sensing elements are bolometers sitting in cavities behind Winston cones. The bandpass of Hertz's filter is centered at 350 μm with $\Delta\lambda/\lambda = 0.1$. In operation at the Caltech Submillimeter telescope, using a half-wave

plate for polarization modulation, Hertz was able to measure polarization with a spatial resolution of 20″ and a precision of 0.3%. Such a precision corresponds to measuring a signal that is 1-2×10^{-6} times the total incident power on the bolometers. (See Appendix.)

6. SUMMARY

We have described a polarimeter that will be a testbed for a new type of modulator that addresses some of the major issues facing the next generation of polarimeters that will be built for wavelengths from the far-infrared through the millimeter. These modulators provide for quantitative systematics assessment, multiple observing wavelengths, and high mechanical reliability.

REFERENCES

1. A. Krabbe, "SOFIA telescope," in *Airborne Telescope Systems*, R. Melugin and H. Roeser, eds., *Proc. SPIE* **4014**, pp. 276–281, June 2000.
2. A. Kosowsky, "The Atacama Cosmology Telescope," *New Astronomy Review* **47**, pp. 939–943, Dec. 2003.
3. P. Padoan, A. Goodman, B. T. Draine, M. Juvela, Å. Nordlund, and Ö. E. Rögnvaldsson, "Theoretical Models of Polarized Dust Emission from Protostellar Cores," *ApJ* **559**, pp. 1005–1018, Oct. 2001.
4. L. Spitzer, *Physical Processes in the Interstellar Medium*, John Wiley & Sons, Inc., New York, 1998.
5. W. Kim, E. C. Ostriker, and J. M. Stone, "Magnetorotationally Driven Galactic Turbulence and the Formation of Giant Molecular Clouds," *ApJ* **599**, pp. 1157–1172, Dec. 2003.
6. F. H. Shu, F. C. Adams, and S. Lizano, "Star formation in molecular clouds - Observation and theory," *ARAA* **25**, pp. 23–81, 1987.
7. N. Evans, "Physical conditions in regions of star formation," *ARAA* **37**, p. 311, 1999.
8. T. Kudoh and K. Shibata, "Magnetically Driven Jets from Accretion Disks. I. Steady Solutions and Application to Jets/Winds in Young Stellar Objects," *ApJ* **474**, p. 362, Jan. 1997.
9. R. M. Crutcher, "Magnetic Fields in Molecular Clouds: Observations Confront Theory," *ApJ* **520**, pp. 706–713, Aug. 1999.
10. A. Lazarian, "Physics of Grain Alignment," in *ASP Conf. Ser. 215: Cosmic Evolution and Galaxy Formation: Structure, Interactions, and Feedback*, p. 69, 2000.
11. J. S. Hall, "Observations of the Polarized Light from Stars," *Science* **109**, pp. 166–167, Feb. 1949.
12. W. A. Hiltner, "Polarization of Light from Distant Stars by Interstellar Medium," *Science* **109**, p. 165, Feb. 1949.
13. W. Cudlip, I. Furniss, K. J. King, and R. E. Jennings, "Far infrared polarimetry of W51A and M42," *MNRAS* **200**, pp. 1169–1173, Sept. 1982.
14. R. H. Hildebrand, M. Dragovan, and G. Novak, "Detection of submillimeter polarization in the Orion nebula," *ApJ* **284**, pp. L51–L54, Sept. 1984.
15. C. D. Dowell, R. H. Hildebrand, D. A. Schleuning, J. E. Vaillancourt, J. L. Dotson, G. Novak, T. Renbarger, and M. Houde, "Submillimeter array polarimetry with Hertz," *ApJ* **504**, pp. 588–598, 1998.
16. M. Houde, C. D. Dowell, R. H. Hildebrand, J. L. Dotson, J. E. Vaillancourt, T. G. Phillips, R. Peng, and P. Bastien, "Tracing the Magnetic Field in Orion A," *ApJ* **604**, pp. 717–740, Apr. 2004.
17. A. Penzias and R. Wilson, "A measurement of excess antenna temperature at 4080 Mc/s," *ApJ* **142**, pp. 419–421, 1965.
18. C. L. Bennett, M. Halpern, G. Hinshaw, N. Jarosik, A. Kogut, M. Limon, S. S. Meyer, L. Page, D. N. Spergel, G. S. Tucker, E. Wollack, E. L. Wright, C. Barnes, M. R. Greason, R. S. Hill, E. Komatsu, M. R. Nolta, N. Odegard, H. V. Peiris, L. Verde, and J. L. Weiland, "First-Year Wilkinson Microwave Anisotropy Probe (WMAP) Observations: Preliminary Maps and Basic Results," *ApJS* **148**, pp. 1–27, Sept. 2003.
19. J. C. Mather, E. S. Cheng, D. A. Cottingham, R. E. Eplee, D. J. Fixsen, T. Hewagama, R. B. Isaacman, K. A. Jensen, S. S. Meyer, P. D. Noerdlinger, S. M. Read, L. P. Rosen, R. A. Shafer, E. L. Wright, C. L. Bennett, N. W. Boggess, M. G. Hauser, T. Kelsall, S. H. Moseley, R. F. Silverberg, G. F. Smoot, R. Weiss, and D. T. Wilkinson, "Measurement of the cosmic microwave background spectrum by the COBE FIRAS instrument," *ApJ* **420**, pp. 439–444, Jan. 1994.

20. J. M. Kovac, E. M. Leitch, C. Pryke, J. E. Carlstrom, N. W. Halverson, and W. L. Holzapfel, "Detection of polarization in the cosmic microwave background using DASI," *Nature* **420**, pp. 772–787, Dec. 2002.
21. A. Cooray, A. Melchiorri, and J. Silk, "is the cosmic microwave background circularly polarized?," *PhB* **554**, pp. 1–6, 2003.
22. D. T. Chuss, S. H. Moseley, G. Novak, and E. J. Wollack, "A Martin-Puplett architecture for polarization modulation and calibration," in *Ground-based Instrumentation for Astronomy*, A. Moorwood and M. Iye, eds., *Proc. SPIE* **5429**, 2004. In these proceedings.
23. D. A. Schleuning, C. D. Dowell, R. H. Hildebrand, and S. R. Platt, "Hertz, a submillimeter polarimeter," *PASP* **109**, pp. 307–318, 1997.
24. R. H. Hildebrand, J. A. Davidson, J. L. Dotson, C. D. Dowell, G. Novak, and J. E. Vaillancourt, "A primer on far-infrared polarimetry," *PASP* **112**, pp. 1215–1235, 2000.
25. G. Novak, D. Chuss, J. Davidson, J. Dotson, C. Dowell, R. Hildebrand, M. Houde, L. Kirby, M. Krejny, A. Lazarian, H. Li, S. Moseley, J. Vaillancourt, and F. Yusef-Zadeh, "A polarimetry module for CSO/SHARC II," in *Millimeter and Submillimeter Detectors for Astronomy II*, J. Zmuidsinas and W. Holland, eds., *Proc. SPIE* **5498**, 2003.
26. C. D. Dowell, C. A. Allen, R. S. Babu, M. M. Freund, M. Gardner, J. Groseth, M. D. Jhabvala, A. Kovacs, D. C. Lis, S. H. Moseley, T. G. Phillips, R. F. Silverberg, G. M. Voellmer, and H. Yoshida, "SHARC II: a Caltech submillimeter observatory facility camera with 384 pixels," in *Millimeter and Submillimeter Detectors for Astronomy*, T. Phillips and J. Zmuidzinas, eds., *Proc. SPIE* **4855**, pp. 73–87, Feb. 2003.
27. T. J. Ames and L. Case, "Distributed framework for dyanmic telescope and instrument control," in *Airborne Telescope Systems II*, R. Melugin and H. Roeser, eds., *Proc. SPIE* **4857**, pp. 73–84, Feb. 2003.

7. APPENDIX: AN ESTIMATE OF THE RATIO OF POLARIZED TO TOTAL POWER ON A POLARIMETRIC PIXEL

In this appendix, we estimate the ratio of polarized to total power on a bolometer using typical conditions for the Hertz polarimeter operating at the Caltech Submillimeter Observatory.[15] find that the time required for integrating a source of flux F_ν to a precision (in polarization) σ_P is

$$t = 0.9\,\mathrm{hour}\left(\frac{50\,\mathrm{Jy}}{F_\nu}\right)^2\left(\frac{0.3\%}{\sigma_P}\right)^2. \tag{1}$$

This equation assumes "good" observing conditions for 350 μm work at Mauna Kea. Even in such conditions $\tau_{350\,\mu m}$=1.4. This means that the sky is radiating a substantial amount onto the bolometers. The question we then ask is what fraction of the total flux on a given bolometer is polarized.

The total Intensity on the bolometers is given by

$$I_\nu = I_{\mathrm{source}}\mathrm{e}^{-\tau_\nu} + B_\nu(T)(1-\mathrm{e}^{-\tau_\nu}). \tag{2}$$

Here, the first term on the right hand side is the contribution from the source and the second term is the contribution from the atmosphere. We define the ratio of these two terms, ζ.

$$\zeta \equiv \frac{I_{\mathrm{source}}}{B_\nu(T)}\frac{\mathrm{e}^{-\tau_\nu}}{(1-\mathrm{e}^{-\tau_\nu})} \tag{3}$$

This is a good approximation for the ratio of source power to total power on the bolometers. We next note that for sky temperatures, we encounter errors of the order of 5% by assuming the Rayleigh-Jeans limit at 350 μm. In addition, we would like to express the intensity from the source in terms of its flux. In this case, we get the following.

$$\zeta = \frac{F_\nu c^2}{2kT\nu^2\Omega}\frac{\mathrm{e}^{-\tau_\nu}}{(1-\mathrm{e}^{-\tau_\nu})} \tag{4}$$

For a typical Hertz observation in good weather, $T = 270K$, $\nu = 857\,GHz$, $\tau_\nu = 1.4$, $\Omega = 7.4 \times 10^{-9} sr$. These values give

$$\zeta_{\text{Hertz}} = 7.3 \times 10^{-6} \left(\frac{F}{Jy} \right) \tag{5}$$

from Equation 1, it can be seen that in a $\sim$1 hour observation, Hertz can measure a 50 Jy source to an precision of 0.3%. Thus, the polarized flux Hertz can measure is 150 mJy. This leads to $\zeta \sim 1.1 \times 10^{-6}$.

A more careful study using numerical integration of the Planck function over the frequency range gives 1.5×10^{-6}.